Air-Core Transformer Integration for GaN VHF Converters*

Ke Xu[1], Zhiliang Zhang[1], Zhi-Wei Xu[1], Jiahua Xu[1], Xiaoyong Ren[1], Qianhong Chen[1] and Fengbing Yu[2]
[1]Aero-Power Sci-Tech Center, Nanjing University of Aeronautics and Astronautics, Jiangsu, P. R. China
[2]Mornsun Company, Guangdong, P. R. China
{xuke, zlzhang, xzwfred, xujh0212, renxy, chenqh}@nuaa.edu.cn and eng400@mornsun.cn

***Abstract*— This paper proposes an air-core transformer integration method, which mounts the transformer straightly into the multi-layer PCB, and maintains the proper distance between the inner transformer and other components on the top layer. Compared with other 3D integration method, the air-core transformer is optimized and modeled carefully to avoid the electromagnetic interference (EMI) of the magnetic fields. The integration method reduces the PCB area significantly, ensuring higher power density and similar efficiency as the conventional planar layout because the air-core transformer magnetic field does not affect other components. Moreover, the converters with the integrated PCB transformer can be manufactured with high consistency. With the air-core transformer, the overall height is only the sum of twice the PCB thickness and components height. In addition, the proposed integration method reduces the power loop inductance by 64%. It is applied to two resonant flyback converters operating at 20 MHz with Si MOSFETs, and 30 MHz with eGaN HEMTs respectively. The full load efficiency of the 30 MHz prototype is 80.1% with 5 V input and 5 V/ 2 W output. It achieves the power density of 32 W/in^3.**

Keywords—air-core transformer; power integration; resonant converter; VHF; eGaN HEMT

I. INTRODUCTION

The converters with small profile and high efficiency are more and more required in industry applications. As the switching frequency goes up, high power density is satisfied. However, there is a limit in power density when the switching frequency reaches a high level [1]-[2]. The power density is mostly influenced by the magnetic components. The structure of inductors and transformers also has effect on the power density. The PCB windings are frequently used in high frequency power converters due to the benefit of high quality factors and low profile. Conventionally, the PCB transformers are integrated tightly to the other components horizontally [3]-[5]. The transformer occupies a large PCB area that impacts the power density. Therefore, it is important to reduce the transformer occupied area to minimize the converter volume. With the great need of the power density, the transformer core is embedded into the PCB to increase the integration density [6]. The power density of a 2 W converter with the switching frequency of 1 MHz reaches 73 W/in^3. However, the transformer is cored so that the magnetic field is constrained. In VHF (30 MHz- 300 MHz) range, the transformers are typically air-cored so that the transformer overall height is only the PCB thickness. Therefore, the VHF converters are suitable for the applications requiring low thickness. However, with the elimination of the magnetic core the magnetic field induced by the air-core transformer spreads widely, causing severe EMI and eddy current in the coppers. So the decoupling design of the transformer and other components is important to the converter efficiency and reliability.

The parasitic inductances are significant in high frequency applications [7]. In VHF range, the parasitic inductances range from several nH to tens of nH, comparable to the resonant inductances. However, the resonant parameters should be precisely controlled to ensure the optimal resonant status and high efficiency. So the parasitic inductances need to be minimized through careful PCB layout.

Enhancement-mode Gallium Nitride high-electron mobility transistors (eGaN HEMTs) are promising in VHF operation due to their faster switching speed and lower Figure of Merit (FOM) compared with the conventional Si MOSFETs [8]-[10]. With the eGaN HEMTs, the efficiency can be further improved.

The contribution of this paper is to propose an air-core transformer integration method in VHF applications. The transformer is integrated into the multi-layer PCB to reduce the occupied area and increase the power density. The method is applied to a 5 V input, 5 V/ 2 W output resonant flyback converter operating at 20 MHz with Si MOSFETs and 30 MHz with eGaN HEMTs respectively.

II. PROBLEMS OF TRANSFORMER IMPLEMENTATION IN VHF RESONANT CONVERTERS

A. Conventional Air-core Transformer Integration Method

At VHF, the magnetic materials are eliminated and magnetic components are simplified to the air-core structures. For frequencies exceeding about 50 MHz, the air-core inductors can offer higher performance at a given size than their magnetic-containing counterparts, with rare exception [11]. Although the air-core transformers have low coupling coefficients, which cause large ratio of the leakage inductance to the magnetizing inductance, the converters power density increases a lot owing to the elimination of the magnetic cores and additional resonant inductors. Conventionally, the air-core transformers are integrated in the main PCB with the other components, which is shown in Fig. 1.

*The work was supported by National Natural Science Foundation of China (51722702, 51377077) and Outstanding Youth Fund of Jiangsu Province.

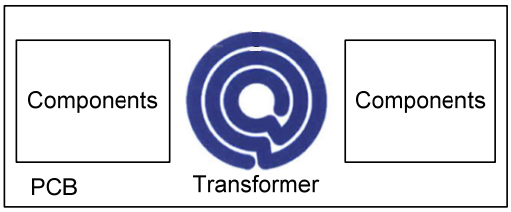

Fig. 1. Conventional air-core transformer integration method

However, the air-core transformer takes a large PCB real estate, which reduces the power density seriously. In addition, the large PCB area results in heavy weight. Since the low volume and light weight is a primary concern in many applications, the air-core transformer should be further integrated. Without the magnetic core, the magnetic field spreads widely and induces the eddy current in the coppers, which causes severe power loss. In addition, the magnetic field may cause severe EMI problems. To avoid two effects, there is a minimum distance between the components and transformer, within which the magnetic mutual effect between the above two parts arises. The distance should be determined with the help of Finite Element Analysis (FEA).

The conventional integration method has another inevitable drawback that if the transformer is spiral, that is, more turns connected in series in one layer, the inner turn is far from the other components. The distance between them induces large parasitic inductance. For VHF converters, the resonant inductances are meant to be precisely controlled since the parasitic inductances that range from several nH to tens of nH may significantly impact the resonant status.

B. *Transformer Design Consideration in VHF Converters*

The air-core transformers design is challenging because the magnetizing and leakage inductances should be precisely controlled. Although the size can be calculated by MATLAB programming, many iterations are still required to obtain the desired inductances. In addition to the inductance requirements, the AC resistance of the windings is of significance because this is the reason for large conduction loss under VHF operation [4]. In general, the wider and shorter the winding is, the smaller the AC resistance is, while the smaller the inductance is. To obtain the desired inductances and low winding loss, the winding structure should be carefully chosen.

III. Proposed Air-core Transformer Integration Method in VHF Resonant Converters

A. *Proposed Air-core Transformer Integration Method*

The proposed transformer integration method is illustrated in Fig. 2. To improve the power density, the transformer is integrated into the lower PCB. The components can be distributed on the top layer of the main PCB without considering the transformer footprint. The distance between the components and the transformer winding is determined by the vertical range of the magnetic field induced by the transformer. The main benefit of this method is the reduction of the PCB area. Since the transformer is coreless, the overall height of the converter is only the sum of the main PCB thickness, the lower PCB thickness and maximum height of other components. The converter power density can be further increased with this method. Moreover, with the design distance between the transformer and other components, the induced magnetic field will not influence the operation of the converter. The efficiency can be similar with that of the conventional structure. Furthermore, this technique is easy to implement and requires no additional process steps in PCB fabrication, ensuring manufacture with high consistency.

The converter components except for the transformer are mounted on the top layer of the upper PCB. The mid layer 1 of the upper PCB is reserved for routing and copper pouring. The mid layer 2 and bottom layer are almost empty except for the pads. The transformer windings are integrated within the lower PCB. The top layer of the lower PCB is empty. The remaining layers are reserved for the transformer windings. So there is almost no copper in the middle of the whole structure, providing a free area for the magnetic field distribution. The distance between two PCBs should be adjusted according to the vertical range of the magnetic field. The PCBs can be connected by pads represented by the conductors in Fig. 2. Furthermore, the transformer windings can be integrated into the main PCB with multi-layers to further increase the power density.

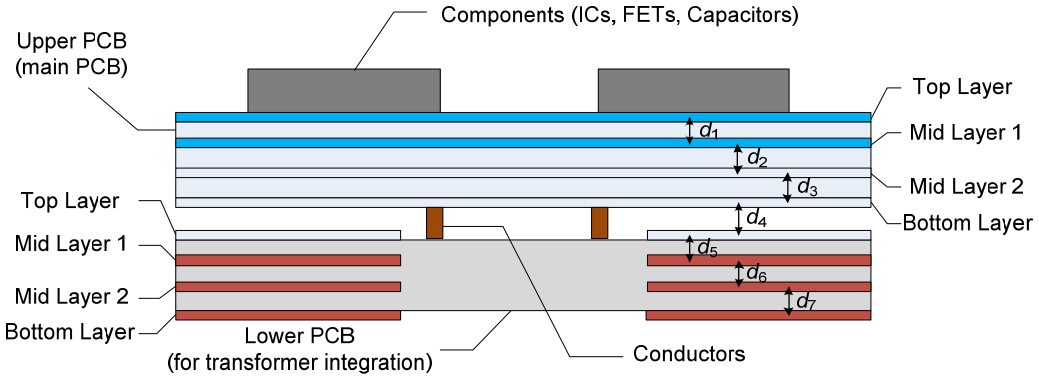

Fig. 2. Proposed air-core transformer integration for VHF resonant converters

B. *Comparison between Conventional and Proposed Transformer Integration Methods*

The sketches of the conventional and proposed transformer integration method are shown in Fig. 3. In Fig. 3(a), the components are coplanar with the transformer. In Fig. 3(b), the transformer windings are integrated beneath the main PCB. The demo circuit is a 2 W resonant flyback converter operating at 20 MHz. A comparison between the PCB layout areas is shown in Fig. 4 (a) and (b). The area of the proposed layout is only 54% of the conventional one.

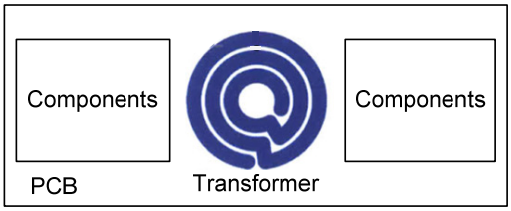

(a) Conventional integration method (top view)

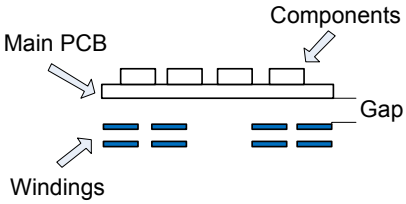

(b) Proposed integration method (side view)

Fig. 3. Sketches of two integration methods

In addition, the proposed method uses the PCB thickness to minimize the power loop formed by the input capacitors, the transformer (T_r) primary winding and power switch, reducing the parasitic inductance significantly compared with the conventional one. The yellow lines, arrows and ⊗/⊙ symbols in Fig. 4 together represent the instantaneous current flow of the power loop. In VHF range, the inductance value is only tens to hundreds of nH, while the parasitic inductance induced by slightly longer PCB wiring could be several nH. With the requirement of precise control of the transformer leakage inductance, the proposed integration method surpasses the conventional one.

Fig. 4 (b) and (c) show the PCB layout of the proposed integration method. The transformer is integrated into an individual PCB that is mounted on the bottom layer of the main PCB. The numbers in Fig. 4 (b) and (c) represent the mounting correspondence between the pads of two individual PCBs.

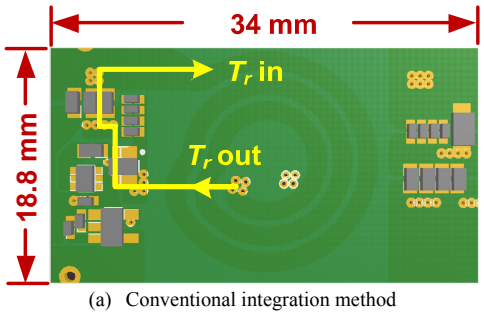

(a) Conventional integration method

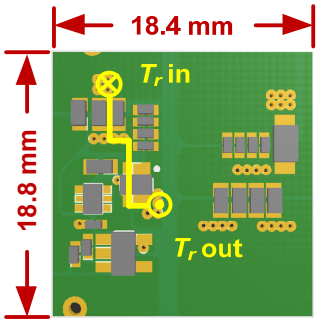

(b) Proposed integration method (top view)

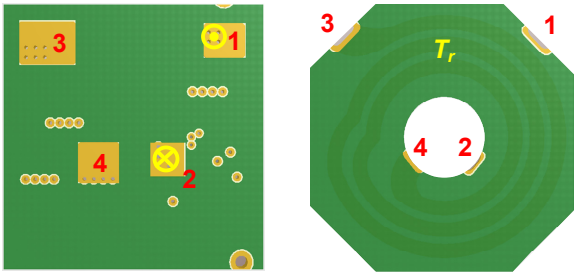

(c) Proposed integration method (bottom view) with PCB air-core transformer separated

Fig. 4. PCB layout comparison between two integration methods

With the aid of Ansys Q3D extractor, the parasitic inductances are extracted and listed in Table I. The parasitic inductance of the proposed method shows a reduction of 64% compared with that of the conventional one. With the advantage of the low parasitic inductance and small PCB area, the proposed integration method is adopted in the following design.

Table I PARASITIC INDUCTANCE COMPARISON BETWEEN TWO METHODS

	Power loop parasitic inductance
Conventional method	9.4 nH
Proposed method	3.4 nH
Reduction	64%

IV. AIR-CORE TRANSFORMER DESIGN OF VHF CONVERTERS

A. *VHF Resonant Flyback Converter*

The proposed air-core transformer integration is applied to a VHF resonant flyback converter. Fig. 5 shows the VHF resonant flyback converter. This converter features high efficiency and excellent transient performance. In addition, the resonant inductors can be eliminated by the use of the air-core transformer. It consists of three parts: the class E inverter, the transformer T_r and class E rectifier [12]-[14]. ZVS of the power switch S_m and ZCS of the diode D_r are realized. The specifications of the converter are listed in Table II. Since the full load power is 2 W, the power density of the converter is a primary priority. The converter with the Si MOSFET operates at 20 MHz, while the converter with the eGaN HEMT operates at 30 MHz.

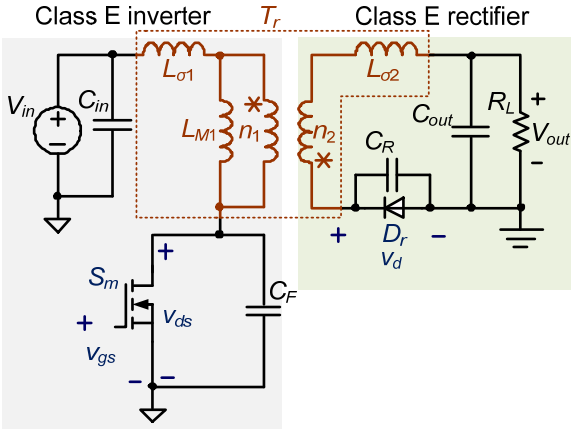

Fig. 5. VHF resonant flyback converter

Table II SPECIFICATIONS OF THE CONVERTER

Input voltage	5 V±10%
Switching frequency	20/30 MHz
Output voltage	5 V±10%
Output current	0.4 A

The detailed design procedure of the power stage is not included due to the limited space, which can be found in [15] and [16]. The following analysis and experimental verification are regarding to the converter in Fig. 5.

B. Selection of Air-core Structure and Simulation of Magnetic Fields

Spiral and helical are two basic structures of the air-core transformers. The spiral structure has several turns connected in series in one layer. The primary side and secondary side are completely separated. The helical structure has several turns connected in series but each turn is in a single layer. The 3D model of two structures are shown in Fig. 6. Since the spiral transformer has more turns in one layer, the turns width is smaller than the helical one with the identical outer diameter, increasing the self-inductance and AC resistance.

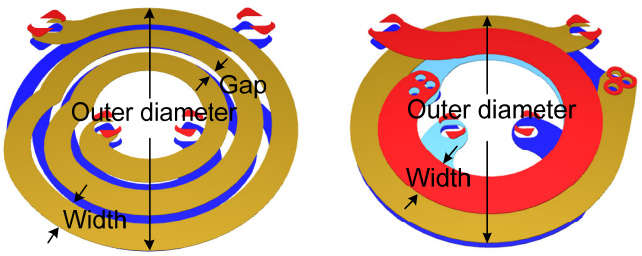

(a) Spiral structure (b) Helical structure

Fig. 6. Transformer 3D model

The air-core transformers are designed in the following manners: 1) Fix the transformer parameters by the converter parameters. 2) Compute the self-inductance of each winding size until it meets the requirements. 3) Compute the mutual inductance of every two windings to find the pairs which meet the self and mutual inductance requirements simultaneously. The computational formulas of the self-inductance and mutual inductances are given in [17]. A MATLAB script is given based on the formulas to determine the specifications of the transformer [11].

A comparison between the spiral and helical structures is made to optimize the transformer efficiency and power density. Take the 20 MHz Si converter as an example, the resonant parameters are designed and the inductance value is included in Table III. The transformer specifications of two structures with the same inductance value are listed in Table IV. The width means the turns width. The gap means the distance between the adjacent windings on the same layer. The copper thickness is 2 oz as a trade-off between the copper loss and the cost. It shows that with the same inductance and turn ratio, the outer diameter of the helical transformer is twice that of the spiral one. The volume of the spiral transformer is much lower than the helical one though the winding loss has an 18% increase. Therefore, the spiral transformer has an advantage over the helical transformer in applications with strict power density requirements.

The transformers of the Si and eGaN converters are designed to be spiral. The primary winding comprises 3 circular turns connected in series in one layer, as well as the secondary winding. The copper thickness is 2 oz. The inductance value and turn ratio are given in Table III. With the increase of the frequency, the inductance value shows a maximum reduction of 47.9%. The detailed geometry parameters are given in Table V. The distance means the vertical distance between the primary winding and secondary winding.

Table III TRANSFORMER PARAMETERS OF SI AND EGAN CONVERTERS

Converter type	L_{M1} (nH)	$L_{\sigma1}$ (nH)	$L_{\sigma2}$ (nH)	n_1:n_2
Si	53	29.2	52.7	1
eGaN	44.3	15.2	36.7	1
Reduction	16.4%	47.9%	30.4%	-

The magnetic fields of both transformers shown in Fig. 7 are extracted by Ansys simulation software. The *P* and *S* represent the primary winding and secondary winding respectively. The current excitation amplitude of the primary side and secondary side are 1.5 A and 1.3 A respectively, which is obtained from the circuit simulation. The maximum flux density exists between the primary and secondary side. The vertical ranges of the magnetic field above the primary winding are 0.6 mm and 0.7 mm respectively. The distance between mid layer 2 of the upper PCB and mid layer 1 of the lower PCB should be larger than the above mentioned magnetic field height, that is: $d_2+ d_3+d_4+ d_5>0.7$ mm.

The design distances among the PCB layers are listed in Table VI. For the Si transformer, the primary winding is on mid layer 1 of the lower PCB and the secondary winding is on bottom layer of the lower PCB. For the eGaN transformer, the primary winding is on mid layer 2 of the lower PCB and the secondary winding is on the bottom layer of the lower PCB.

Table IV TRANSFORMER SPECIFICATIONS OF TWO STRUCTURES

Structure	Side	Turn number	Outer diameter/mm	Width/mm	Gap/mm	Volume/mm^3	Winding loss/mW
Spiral	Primary	3	17.5	1.5	0.5	368	184
	Secondary	3	16.8	1.0	0.5		
Helical	Primary	2	35	2.4	-	1470	150
	Secondary	2	28	2.5	-		
Increase	-	-	-	-	-	400%	-18%

Table V TRANSFORMER SPECIFICATIONS OF SI AND EGAN CONVERTERS

Converter type	Side	Turn number	Outer diameter/mm	Width/mm	Gap/mm	Distance/mm
Si	Primary	3	17.5	1.5	0.5	1
	Secondary	3	16.8	1.0	0.5	
eGaN	Primary	3	16.1	1.5	0.5	0.5
	Secondary	3	16.0	1.0	0.5	

Table VI PCB LAYER DISTANCE DESIGN

Distance	d_1/d_5	d_2/d_6	d_3/d_7	d_4
Value/mm	0.2	0.5	0.5	0

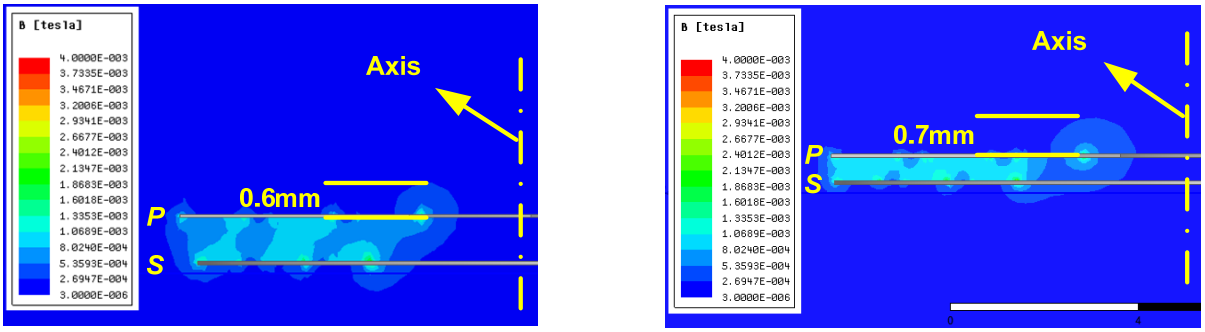

(a) 20 MHz Si converter (b) 30 MHz eGaN converter

Fig. 7. Simulated transformer magnetic field

V. EXPERIMENTAL RESULTS AND DISCUSSION

Two 5 V input, 5 V/ 0.4 A output resonant flyback converters with the frequency of 20 MHz and 30 MHz respectively were built to verify the effectiveness of the proposed transformer integration method.

A. 20 MHz Si Resonant Converter With Proposed Transformer Integration Method

The parameters of the power stage are just given in Table VII. The photos of the prototype are shown in Fig. 8. The Si MOSFET, diode, capacitors and ICs are mounted on the top layer, which is shown in Fig. 8 (a). Fig. 8 (b) shows the air-core transformer PCB windings mounted on the bottom layer of the main PCB. The overall height of the converter is only 3.4 mm, which is shown in Fig. 8 (c). The gate drive signal is produced by the 33 MHz oscillator LTC1799 and enhanced by the dual BUFFER NC7WZ17.

Table VII POWER STAGE COMPONENT VALUE OF 20 MHZ SI PROTOTYPE

L_{M1}	53 nH	D_r	PMEG3010ER (NXP, 30 V, 1 A)
$L_{\sigma 1}$	29.2 nH	C_F	450 pF
$L_{\sigma 2}$	52.7 nH	C_r	270 pF
C_{in}	4.7 μF×2	n_1	3
C_{out}	10 μF×2	n_2	3
S_m	BSD316SN (Infineon, 30 V, 1.4 A)		

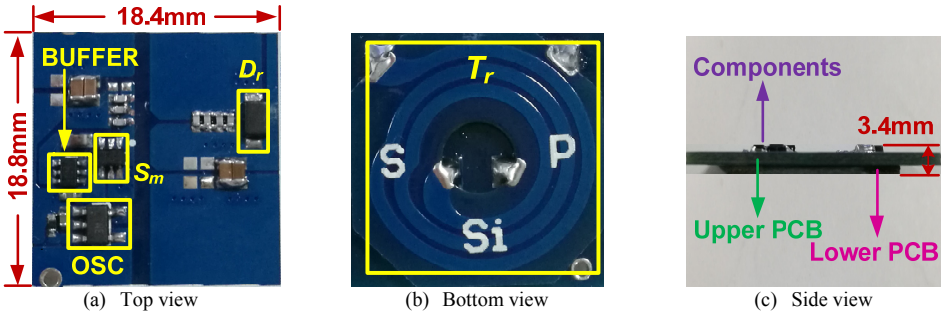

(a) Top view (b) Bottom view (c) Side view

Fig. 8. Photos of 20 MHz Si prototype with proposed transformer integration method

The waveforms of v_{gs} and v_{ds} are shown in Fig. 9. S_m achieves ZVS and the turn-on loss is minimized. Since the hard gating loss of the Si MOSFET is large (2.5% of the full load power), the resonant gate driver is used in this example, saving 40% of the hard gating loss. The waveform of v_d is shown in Fig. 10. The power losses measured by the thermal imager are shown in Fig. 11. The transformer loss is much larger than other types of loss. The full load efficiency is tested to be 79% with 5 V input and 2 W output, showing 1.9% discrepancy from the calculated value. The power density is 28 W/in^3.

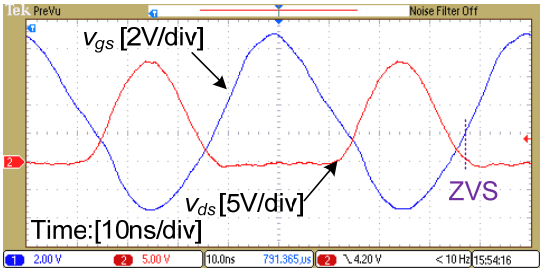

Fig. 9. Waveforms of v_{gs} and v_{ds}: V_{in}= 5 V, P_{out}=2 W and f_s=20 MHz

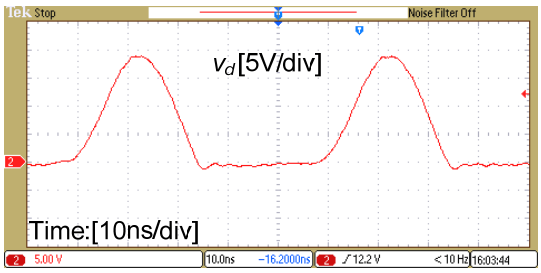

Fig. 10. Waveforms of v_d: V_{in}= 5 V, P_{out}=2 W and f_s=20 MHz

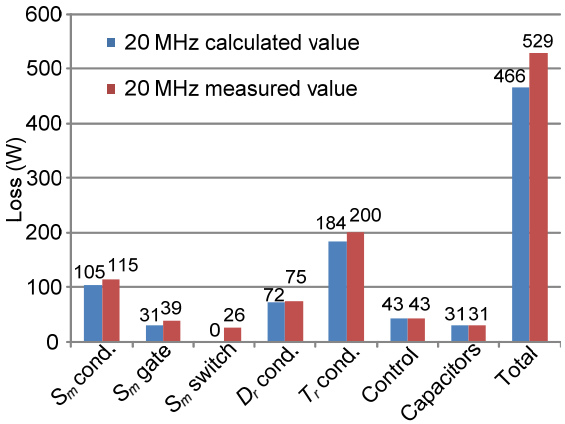

Fig. 11. Loss breakdown of Si prototype: V_{in}= 5 V, P_{out}=2 W and f_s=20 MHz

B. *30 MHz eGaN Resonant Converter With Proposed Transformer Integration Method*

The parameters of the power stage are just given in Table VIII. The photos of the prototype are shown in Fig. 12. The integration structure is the same as the Si prototype.

Table VIII POWER STAGE COMPONENT VALUE OF 30 MHZ EGAN PROTOTYPE

L_{M1}	44.3 nH	D_r	PMEG3010ER (NXP, 30 V, 1 A)
$L_{\sigma 1}$	15.2 nH	C_F	220 pF
$L_{\sigma 2}$	36.7 nH	C_r	100 pF
C_{in}	4.7 μF×2	n_1	3
C_{out}	10 μF×2	n_2	3
S_m	EPC8004 (EPC, 40 V, 2.7 A)		

(a) Top view (b) Bottom view (c) Side view

Fig. 12. Photos of 30 MHz eGaN prototype with proposed transformer integration method

The waveforms of v_{gs} and v_{ds} are shown in Fig. 13. The eGaN HEMT S_m achieves ZVS and the turn-on loss is minimized. The waveform of v_d is shown in Fig. 14.

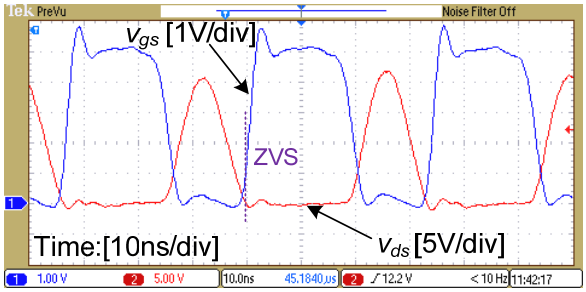

Fig. 13. Waveforms of v_{gs} and v_{ds}: V_{in}= 5 V, P_{out}=2 W and f_s=30 MHz

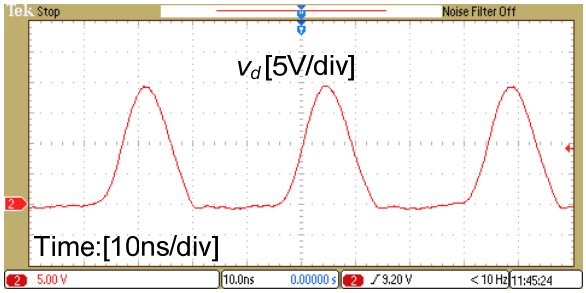

Fig. 14. Waveforms of v_d: V_{in}= 5 V, P_{out}=2 W and f_s=30 MHz

The 30 MHz eGaN prototype achieves the full load efficiency of 80.1% at 5 V input and 2 W output, an improvement of 1% compared with the 20 MHz Si prototype due to the reduction of S_m and T_r conduction loss. The power density is 32 W/in^3, an improvement of 14% compared with the 20 MHz Si prototype. Fig. 15 shows the loss breakdown comparison between the calculated and measured value of the eGaN prototype. The full load efficiency and power density of the Si and eGaN prototypes are listed in Table IX.

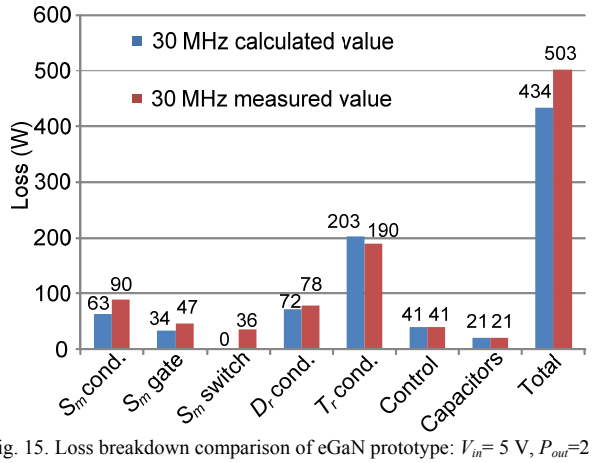

Fig. 15. Loss breakdown comparison of eGaN prototype: V_{in}= 5 V, P_{out}=2 W, and f_s=30 MHz

Table IX Full Load Efficiency and Power Density Comparison

Prototype	Efficiency at 5 V input		Power density		Weight	
	Value (%)	Improvement (%)	Value (W/in^3)	Improvement (%)	Value (g)	Reduction (%)
20 MHz Si	79	-	28	-	1.99	-
30 MHz eGaN	80.1	1.1	32	14	1.82	8.5

The full load efficiency with different V_{in} is shown in Fig. 16. Since the proportional variation of the output voltage according to the input voltage leads the gate drive voltage to match well with the drain voltage of the power FETs with the rated load in the open-loop status [18], the variation of the efficiency is within 2%.

The converters with the proposed transformer integration method are compared with some commercial products. The results are shown in Fig. 17. The converters in this paper show a maximum 45% improvement on the power density compared with other products with the VHF technique and proposed transformer integration method. The use of eGaN HEMT also improves the efficiency when the frequency increases from 20 MHz to 30 MHz. The 20 MHz and 30 MHz converters overall height shows a maximum reduction of 60%, listed in Table X.

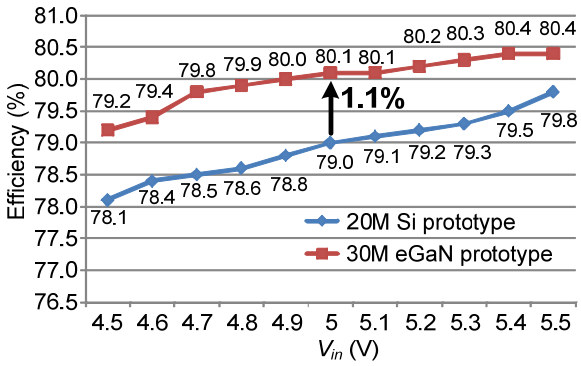

Fig. 16. Full load efficiency with different V_{in}

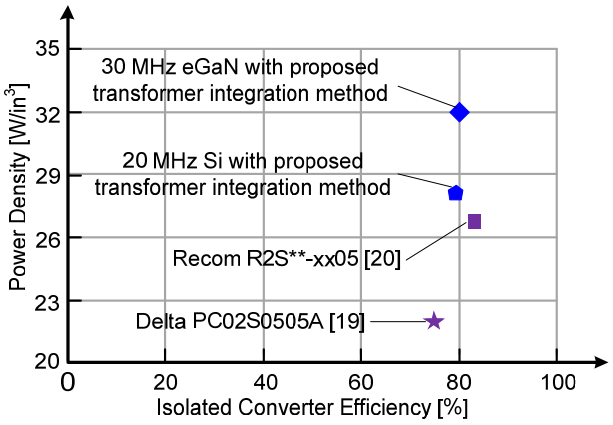

Fig. 17. Power density and efficiency comparison with commercial products

Table X OVERALL HEIGHT COMPARISON BETWEEN VHF CONVERTERS AND COMMERCIAL PRODUCTS

Part Number	Overall Height	Maximum Reduction
PC02S0505A	7.6 mm	-
R2S**-xx05	8.7 mm	-
20 M/ 30 M Converters	3.4 mm	60%

VI. CONCLUSIONS

A transformer integration method is proposed. The air-core transformer is integrated into the multi-layer PCB to reduce the occupied area by 46% and improve the power density. In addition, the parasitic inductance of the power loop has a decrease of 64% with the proposed integration method. The distance between the transformer winding and other components is controlled with Ansys simulation software to avoid the magnetic mutual effects. The spiral and helical transformer structures are compared to choose the suitable one to improve the power density. The transformer integration method is applied to a resonant flyback converter with 5 V input, 5 V/ 2 W output operating at 20 MHz with the Si MOSFET, and 30 MHz with the eGaN HEMT respectively. The 30 MHz prototype with the eGaN HEMT achieves the full load efficiency of 80.1 % (an increase of 1.1% compared with the Si prototype) at 5 V input, 2 W output and power density of 32 W/in^3 (an increase of 14% compared with the Si prototype). With the proposed air-core transformer integration method, the VHF resonant converters in this paper show a maximum 45% improvement on the power density compared with the commercial products. Moreover, the overall height is only 3.4 mm, half of the commercial products. So the VHF converters are suitable for the applications requiring low thickness.

References

[1] W. Odendaal and J. Ferreira, "Effects of scaling high-frequency transformer parameters," *IEEE Transactions on Industry Applications.*, vol. 35, pp. 932–940, Jul/Aug 1999.

[2] W. J. Gu and R. Liu, "A study of volume and weight vs. frequency for high-frequency transformers," *24th Annual IEEE Power Electronics Specialists Conference*., pp. 1123–1129, Jun 1993.

[3] A. Sepahvand, Y. Zhang, and D. Maksimovic, "100 MHz isolated DC-DC resonant converter using spiral planar PCB transformer," in *Proc. IEEE Workshop Contr. Modl. Pwr. El.*, Jul 2015.

[4] Z. Zhang, Z. Dong, X. Zou and X. Ren, "A digital adaptive driving scheme for eGaN HEMTs in VHF converters," *IEEE Trans. Power Electron*., vol. 32, no. 8, pp. 6197-6205, Aug. 2017.

[5] X. Ren, Y. Zhou, W. Dong, X. Zou, and Z. Zhang, "A 10-MHz isolated synchronous class-Φ_2 resonant converter," *IEEE Trans. Power Electron*., vol. 31, no. 12, pp. 8317-8328, Dec. 2016.

[6] B. Sun, R. Burgos, D. Boroyevich, R. Perrin, C. Buttay, B. Allard, N. Quentin, and M. Ali, "Two comparison-alternative high temperature PCB-embedded transformer designs for a 2 W gate driver power supply," in *Proc. IEEE Energy Convers. Congr. Expo*., 2016, pp. 1-7.

[7] D. Reusch and J. Strydom, "Understanding the effect of PCB layout on circuit performance in a high frequency GaN based point of load converter," *IEEE Trans. Power Electron*., vol. 29, no. 4, pp. 2008-2015, Apr. 2014.

[8] A. Lidow, J. Strydom, M. D. Rooij, and D. Reusch, "GaN transistors for efficient power conversion," 2nd ed., *John Wiley & Sons*, 2014.

[9] A. Lidow, D. Reusch, and J. Strydom, "GaN integration for higher DC-DC efficiency and power density," Application Note, EPC Co., 2015.

[10] D. Reusch and J. Strydom, "Evaluation of gallium nitride transistors in high frequency resonant and soft-switching DC-DC converters," *IEEE Trans. Power Electron.*, vol. 30, no. 9, pp. 5151-5158, 2015.

[11] A. D. Sagneri, "Design of miniaturized radio-frequency dc-dc power converters," Ph.D. dissertation, Massachusetts Institute of Technology, Cambridge, MA, Feb. 2012.

[12] T. W. Barton, J. M. Gordonson, and D. J. Perreault, "Transmission line resistance compression networks and applications to wireless power transfer," *IEEE J. Emerg. Sel. Top. Power Electron.*, vol. 3, no. 1, pp. 252–260, Mar. 2015.

[13] A. Ivascu, M. K. Kazimierczuk, and S. Birca-Galateanu, "Class E resonant low dv/dt rectifier," *IEEE Trans. Circuits Syst*., vol. 39, no. 8, pp. 604–613, Aug. 1992.

[14] S. Aldhaher, P. C. K. Luk, K. E. K. Drissi, and J. F. Whidborne, "High-input-voltage high-frequency class E rectifiers for resonant inductive links," *IEEE Trans. Power Electron*., vol. 30, no. 3, pp. 1328–1335, Mar. 2015.

[15] J. M. Rivas, Y. Han, O. Leitermann, A. D. Sagneri, and D. J. Perreault, "A high-frequency resonant inverter topology with low-voltage stress," *IEEE Trans. Power Electron.*, vol. 23, no. 4, pp. 1759-1771, 2008.

[16] R. Pilawa-Podgurski, A. D. Sagneri, J. M. Rivas, D. I. Aderson, and D. J. Perreault, "Very high frequency resonant boost converter," *IEEE Trans. Power Electron.*, vol. 24, no. 6, pp. 1654-1665, 2009.

[17] W. G. Hurley and M. C. Duffy. "Calculation of self and mutual impedances in planar magnetic structures," *IEEE Transactions on Magnetics*., vol. 31, no. 4:2416-2422, 1995.

[18] Z. Zhang, X. Zou, Z. Dong, Y. Zhou, and X. Ren, "A 10-MHz eGaN isolated class-Φ_2 DCX," *IEEE Trans. Power Electron*., vol. 32, no. 3, pp. 2029–2040, Mar. 2017.

[19] Delta, PC02S0505A. [Online] Available: http://13.76.185.95/filecenter/Products/download/01/0102/datasheet/DS_PC02S_D.pdf

[20] Recom, R2S**-xx05, (2015). [Online] Available: https://www.recom-power.com/ pdf/Econoline/R2S_R2D.pdf